

Performance of a multi-story structure with a resilient-friction base isolation system

Won-Kee Hong ^{*}, Hee-Cheul Kim ¹

Department of Architectural and Civil Engineering, Kyung Hee University, Kyungki-do 449-701, Korea

Received 6 May 2002; accepted 7 June 2004

Abstract

Complex frequency response functions and excitation–response relations for stationary random process are formulated to estimate responses of multi-story superstructures isolated with resilient-friction base isolation (R-FBI) system. The equivalent linearization technique is also used to linearize the nonlinear governing equations of motion of R-FBI system occurred between the parallel actions of the resiliency of rubber and friction of Teflon-coated plates. In this approach, the spectral density functions for both the relative displacement response and absolute acceleration response of N degrees of freedom systems are derived. The applicability and accuracy of the proposed methodology are examined by comparing the resulting responses obtained from this study with those calculated from time history analysis based method. These two studies demonstrate good agreement in terms of characteristics of peak responses. Extensive sensitivity analysis to find the influence of various important structural parameters on the behavior of structures isolated with R-FBI system is also carried out.

© 2004 Elsevier Ltd. All rights reserved.

Keywords: Base isolation; Frequency domain; Stochastic linearization; Relative displacement response spectral density; Absolute acceleration response spectral density; Wiener–Khinchine relation

1. Introduction

Seismic isolation in ordinary buildings has been successively adapted to provide flexibility for the reduction of base shear forces. Implementing the innovative concept to multi-story buildings requires both understanding and predicting the characteristics of isolators as well as the behavior of cushioned superstructures.

Mostaghel [1–3] proposed the resilient-friction isolator consisting of concentric layers of Teflon-coated plates that provide friction during the seismic activity. A core of laminated rubber bearing provides base isolation through the parallel action of friction, damping as well as restoring springs. Su et al. [4] developed a new base isolator referred to as the sliding resilient-friction (SR-F) base isolation system by replacing the elastomeric bearings of the Electricite de France (EDF) base isolation system [5] by the resilient-friction base isolation (R-FBI) system. Su and Tadjbakhsh [6] also investigated performances of the SR-F base-isolated structures which are modeled as nonuniform shear frame subjected to several earthquakes and sinusoidal input motion with the amplitude of 0.6g.

^{*} Corresponding author. Tel.: +82 31 201 2069; fax: +82 31 202 2107.

E-mail addresses: hongwk@khu.ac.kr (W.-K. Hong), kimhc@khu.ac.kr (H.-C. Kim).

¹ Tel.: +82 31 201 2542; fax: +82 31 202 2107.

Booton [7], Kazakov [8], and Caughey [9] developed the equivalent linearization technique. Spanos [10] extended the application of the technique to relatively large nonlinearities. Caughey [11,12] proposed that a general nonlinear system can be replaced by a special equivalent linear system when the exact stationary response probability density function is known. Su and Ahmadi [13] studied a rigid structure with a frictional base isolation system subjected to random earthquake excitation. Fan and Ahmadi [14] carried the response analysis of a randomly excited nonlinear system based on equivalent linearization technique and stochastic averaging method. Lin et al. [15] compared the performances of three different base-isolation system in which the equivalent linearization technique is used to linearize the nonlinear governing equations of motion. In Lin's work, the effective frequency of the entire system is obtained by assuming that the superstructure behaves like a rigid body. Constantinou and Tadjbakhsh [16] studied response of a sliding structure to filtered random excitation. In 1990, Papageorgiou and Constantinou [17] investigated response of sliding structures with restoring force to stochastic excitation. Basu [20] proposed a wavelet-based stochastic formulation for the seismic analysis of a base-isolated structural system which is modelled as a two-degree-of-freedom (2-DOF) system. The ground motion has been modelled as a nonstationary process (both in amplitude and frequency) by using modified Littlewood–Paley basis wavelets. Basu's formulation is based on replacing the nonlinear system by an equivalent linear system with time-dependent damping properties. The expressions of the instantaneous damping and the power spectral density function (PSDF) of the superstructure response have been obtained in terms of the functions of input wavelet coefficients. Khechfe et al. [21] provide an experimental study on the feasibility of base isolation for seismic protection of nonstructural secondary system. A one-sixth-scaled three-story building model with a single-degree-of-freedom secondary system placed on its third floor is employed. The secondary system is base-isolated by a laminated rubber bearing (LRB) base isolation system from the supporting floor. The ground motion input is simulated by a shaking table which generates three different types of signal including sweeping harmonic sinusoidal, the S00E component of the 1940 El Centro earthquake, and the simulated white noise.

In this study, the response statistics of a structure isolated with the resilient-friction base isolator are evaluated by linearization approximation. Extensive computational effort and time is necessary to study the behavior of base-isolated structure based on conventional time history analysis. In this paper, responses of multi-story superstructures isolated with resilient-friction base isolation (R-FBI) system are calculated based

on complex frequency response functions and excitation–response relations for stationary random process, leading to considerable reduction in computational time. Peak responses of the structure subjected to seismic acceleration of the modified Clough–Penzien power spectrum are then evaluated. Equivalent linearization process is employed for the linearization of the nonlinear governing equations that come from R-FBI system consisted of the parallel actions of the resiliency of rubber and friction of Teflon-coated plates. From the transfer functions found from the linearized governing equations, the responses of interest including mean square relative displacements of lumped masses with respect to foundation and mean square absolute accelerations of lumped degrees of freedom are calculated as a function of system parameters for both fixed and isolated base conditions. The responses of both fixed and isolated structures obtained from the analysis method based on frequency domain are used to compare the two different behaviors. Finally the sensitivity analysis of performance of resilient-friction base isolation system to various structural parameters is carried out and the results obtained from the analysis of frequency domain are compared and verified with the study performed by Su and Tadjbakhsh [6].

2. Equations of motion and equivalent linearization technique

An analytical model for a multi-story structure with the resilient-friction base isolator (R-FBI) system is described in Fig. 1(a) and (b). Superstructure is modeled as planar liner system with classical damping by Lin et al. [15]. Base isolation system is installed between foundation and the basement of a superstructure as shown in Fig. 1(a). Schematic diagram of a rigid structure with the resilient-friction base isolator is shown in Fig. 1(b). The governing equations of motion for the structures isolated with resilient-friction base isolator are formulated based on the method of equivalent linearization developed by Caughey [9] since the response of the structure isolated with R-FBI system is nonlinear. Lin et al. [15] and Fan et al. [14] formulated approximate solution to the nonlinear response of a structure with R-FBI system for a multi-story, lumped mass, shear type building. The formulation of mathematical equations of motion can be derived from the schematic diagram of R-FBI system as shown Fig. 1(a) and (b). The equations of motion for the superstructure can be written as in Eq. (1) in which $[M]$, $[C]$, and $[K]$ are the mass, damping, and stiffness matrices of superstructure, respectively.

$$[M]\{\ddot{y}\} + [C]\{\dot{y}\} + [K]\{y\} = -[M]\{1\}(\ddot{y}_b + \ddot{y}_g) \quad (1)$$

where,

$$\sigma_{\dot{y}_b} = \frac{\left[\frac{2}{\pi} (1 + N\alpha)^2 \mu'^2 g^2 + 8\xi_b \omega_b \pi G_0 \right]^{\frac{1}{2}} - \left(\frac{2}{\pi} \right) (1 + N\alpha) \mu' g}{4\xi_b \omega_b} \quad (8)$$

G_0 is the spectral density of excitation for white noise excitation. Since standard deviation $\sigma_{\dot{y}_b}$ is time-dependent, ξ_e is also time-dependent. ξ_e becomes constant, however, when the standard deviation $\sigma_{\dot{y}_b}$ reaches stationariness in a very short time.

3. Response of base isolated multi-story structures to stationary random excitation

3.1. Complex frequency responses

The excitation described by its acceleration $\ddot{y}_g(t)$ is applied to foundation. The present study examines a total of $3(N + 1)$ responses including $(N + 1)$ relative displacements (y_1, \dots, y_n, y_b) and the absolute acceleration of the $(N + 1)$ masses $(\ddot{y}'_1, \ddot{y}'_2, \dots, \ddot{y}'_n, \ddot{y}'_b)$ and the $(N + 1)$ velocity at each degree of freedom. The quantities \ddot{y}'_i, \ddot{y}'_b are the accelerations of the $(N + 1)$ masses with respect to the base and the ground, respectively. There are $3(N + 1)$ complex frequency responses, $H_{y_1}(\omega), H_{\dot{y}_1}(\omega), H_{\ddot{y}_1}(\omega), H_{y_2}(\omega), H_{\dot{y}_2}(\omega), H_{\ddot{y}_2}(\omega), \dots, H_{y_n}(\omega), H_{\dot{y}_n}(\omega), H_{\ddot{y}_n}(\omega), H_{y_b}(\omega), H_{\dot{y}_b}(\omega), H_{\ddot{y}_b}(\omega)$. Upon substituting these input–output relationships in terms of complex frequency responses into the equations of motion, shown in Eqs. (1)–(3), the following linearized equations (9) and (10) are established.

$$(\omega^2 - \omega_n^2)H_{v_n}(\omega) - 2\xi_n \omega_n (i\omega)H_{v_n}(\omega) + \omega_n^2 H_{v_{n-1}}(\omega) + \omega_n^2 H_{v_{n-1}}(\omega) + 2\xi_n \omega_n (i\omega)H_{v_{n-1}}(\omega) + \omega^2 H_{v_n}(\omega) = 1 \quad (9)$$

$$\begin{aligned} &\mu_n \omega_n^2 H_{y_n}(\omega) + 2\xi_n \omega_n (i\omega) \mu_n H_{y_n}(\omega) + (\omega_n^2 - \omega_{n-1}^2 - \omega_n^2 \mu_n) \\ &\times H_{y_{n-1}}(\omega) - (2\xi_{n-1} \omega_{n-1} + 2\xi_n \omega_n \mu_n) (i\omega) H_{y_n}(\omega) \\ &- (\omega) + \omega_n - 1^2 H_{y_{n-2}}(\omega) + 2\xi_{n-1} \omega_{n-1} (i\omega) H_{y_{n-1}} \\ &+ \omega^2 H_{y_n}(\omega) = 1 \end{aligned} \quad (10)$$

where,

$$\begin{aligned} \mu_1 &= \alpha_1 = \frac{m_1}{m_b}, \quad \mu_2 = \alpha_2 = \frac{m_1}{m_2}, \quad \mu_3 = \alpha_3 = \frac{m_2}{m_3}, \\ \dots, \quad \mu_{n-1} &= \alpha_{n-1} = \frac{m_{n-2}}{m_{n-1}}, \quad \mu_n = \alpha_n = \frac{m_{n-1}}{m_n} \end{aligned}$$

These equations can be rewritten in matrix form as shown in Eq. (11).

$$[\omega^*] \begin{Bmatrix} H_y \end{Bmatrix} = [I] \quad (11)$$

$(n+1)(n+1) \quad (n+1)(1) \quad (n+1)(1)$

where $\{H_y\}^T = \{H_{y_b}, H_{y_1}, H_{y_2}, H_{y_3}, \dots, H_{y_{n-1}}, H_{y_n}\}$.

The absolute accelerations at each degree of freedom under consideration, are $\ddot{y}'_1, \ddot{y}'_2, \dots, \ddot{y}'_n$, and shown in Eq. (12).

$$\ddot{y}'_i = \ddot{y}_g + \ddot{y}_b + \ddot{y}_i \quad \text{for } i = 1, \dots, n \quad (12)$$

The absolute acceleration at the isolator is also given by Eq. (13).

$$\ddot{y}'_b = \ddot{y}_g + \ddot{y}_b \quad (13)$$

Rearranging the linearized system equations in terms of acceleration and combining them with complex frequency responses yield Eq. (14).

$$[M]\{\ddot{y} + \ddot{y}_b + \ddot{y}_g\} + [C]\{\dot{y}\} + [K]\{y\} = 0 \quad (14)$$

and, Eq. (15) is obtained from Eq. (3).

$$\begin{aligned} &(\ddot{y}_b + \ddot{y}_g) + 2(\xi_b + \xi_e) \omega_b \dot{y}_b + \omega_b^2 y_b - 2\xi_1 \omega_1 \alpha \dot{y}_1 \\ &- \omega_1^2 \alpha y_1 = 0 \end{aligned} \quad (15)$$

Eqs. (14) and (15) apply to superstructure and base, respectively.

The term, $\{\ddot{y} + \ddot{y}_b + \ddot{y}_g\}$ in Eq. (14) can be modeled as $e^{i\omega t} \{H_{\ddot{y}}\}$ in terms of complex frequency of absolute acceleration responses where $\{H_{\ddot{y}}\}^T = \{H_{\ddot{y}_1}, H_{\ddot{y}_2}, H_{\ddot{y}_3}, \dots, H_{\ddot{y}_{n-1}}, H_{\ddot{y}_n}\}$ and also the first term in Eq. (15) can be expressed as $e^{i\omega t} \{H_{\dot{y}_b}\}$.

Substituting these relationships and the input–output relationships in terms of complex frequency responses into Eqs. (14) and (15) provides the following relationships.

$$\begin{aligned} H_{\ddot{y}_{n-1}} &= -\omega_n^2 H_{y_n}(\omega) - 2\xi_n \omega_n (i\omega) H_{y_n}(\omega) \\ &+ \omega_n^2 H_{y_{n-1}}(\omega) + 2\xi_n \omega_n (i\omega) H_{y_{n-1}}(\omega) \end{aligned} \quad (16)$$

$$\begin{aligned} H_{\ddot{y}_{n-1}} &= \mu_n \omega_n^2 H_{y_n}(\omega) + 2\xi_n \omega_n (i\omega) \mu_n H_{y_n}(\omega) \\ &- (\omega_{n-1}^2 + \omega_n^2 \mu_n) H_{y_{n-1}}(\omega) - (2\xi_{n-1} \omega_{n-1} \\ &+ 2\xi_n \omega_n \mu_n) (i\omega) H_{y_{n-1}}(\omega) + \omega_{n-1}^2 H_{y_{n-2}}(\omega) \\ &+ 2\xi_{n-1} \omega_{n-1} (i\omega) H_{y_{n-2}}(\omega) \end{aligned} \quad (17)$$

...

$$\begin{aligned} H_{\ddot{y}_2} &= \mu_3 \omega_3^2 H_{y_3}(\omega) + 2\xi_3 \omega_3 (i\omega) \mu_3 H_{y_3}(\omega) \\ &- (\omega_2^2 + \omega_3^2 \mu_3) H_{y_2}(\omega) - (2\xi_2 \omega_2 + 2\xi_3 \omega_3 \mu_3) \\ &\times (i\omega) H_{y_2}(\omega) + \omega_2^2 H_{y_1}(\omega) + 2\xi_2 \omega_2 (i\omega) H_{y_1}(\omega) \end{aligned} \quad (18)$$

$$\begin{aligned} H_{\ddot{y}_1} &= \mu_2 \omega_2^2 H_{y_2}(\omega) + 2\xi_2 \omega_2 (i\omega) \mu_2 H_{y_2}(\omega) \\ &- (\omega_1^2 + \omega_2^2 \mu_2) H_{y_1}(\omega) - (2\xi_1 \omega_1 + 2\xi_2 \omega_2 \mu_2) \\ &\times (i\omega) H_{y_1}(\omega) \end{aligned} \quad (19)$$

$$\begin{aligned} H_{\ddot{y}_b} &= \mu_1 \omega_1^2 H_{y_1}(\omega) + 2\xi_1 \omega_1 (i\omega) \mu_1 H_{y_1}(\omega) \\ &- \omega_b^2 H_{y_b}(\omega) - 2\omega_2 (\xi_e + \xi_b) (i\omega) H_{y_b}(\omega) \end{aligned} \quad (20)$$

These can be rewritten in terms of matrix form as follows.

$$\begin{bmatrix} \omega^{**} \\ (n+1)(n+1) \end{bmatrix} \{ H_y \}_{(n+1)(1)} = \begin{bmatrix} H_{\ddot{y}} \\ (n+1)(1) \end{bmatrix} \quad (21)$$

Substituting Eq. (11) into these relationships, the complex frequency response functions of acceleration, $\{H_{\ddot{y}}\}$ can be computed.

If the mean square spectral density of an output process is expressed as $S_x(\omega)$ then Wiener–Khinchine [19] relation becomes

$$S_x(\omega) = \frac{1}{2\pi} \int_{-\infty}^{\infty} R_x(\xi) e^{-i\omega\xi} d\xi \quad (22)$$

A slightly more compact form of Eq. (23) is achieved by noting that the product of $H(\omega)$ and its complex conjugate may be written as the square of the magnitude of $H(\omega)$. The power spectra of both displacement and acceleration are obtained as shown in Eqs. (24) and (25) when ground motion can be represented by the ideal white noise spectrum of constant density S_0 .

$$S_y(\omega) = H(-\omega)H(\omega)S_x(\omega) \quad (23)$$

$$\Phi_g(f) = S_0 \left\{ \frac{1 + 4\zeta_g^2 \left(\frac{f}{f_g}\right)^2}{\left[1 - \left(\frac{f}{f_g}\right)^2\right]^2 + 4\zeta_g^2 \left(\frac{f}{f_g}\right)^2} \right\} \left\{ \frac{\left(\frac{f}{f_c}\right)^4}{\left[1 - \left(\frac{f}{f_c}\right)^2\right]^2 + 4\zeta_c^2 \left(\frac{f}{f_c}\right)^2} \right\} \left\{ \frac{1}{\left[1 - \left(\frac{f}{f_m}\right)^2\right]^2 + 4\zeta_m^2 \left(\frac{f}{f_m}\right)^2} \right\} \quad (27)$$

$$S_y(\omega) = |H(\omega)|^2 S_x(\omega) \quad (24)$$

$$S_y(\omega) = |H(\omega)|^2 S_0 \quad (25)$$

where $S_y(\omega)$ is the mean square response power spectrum and S_0 is the mean square acceleration in rad/s. This is the desired relation between the spectral density of the excitation $x(t)$ and the spectral density of response $y(t)$. In case that the ground excitation is assumed to have zero mean stationary value, the responses are also zero mean processes with the corresponding variances, as shown in Eqs. (26) and (27).

$$\begin{aligned} E[y^2] &= \int_{-\infty}^{\infty} S_y(\omega) d\omega \\ &= \int_{-\infty}^{\infty} \{|H(\omega)|^2 S_x(\omega)\} d\omega \\ &= S_0 \int_{-\infty}^{\infty} \{|H(\omega)|^2\} d\omega \end{aligned} \quad (26)$$

$$\sigma = \sqrt{E[y^2]}$$

3.2. Earthquake input motions

The realistic input ground motions with moment magnitude of 7.3 are used to evaluate the performance of the base-isolated structures. The modified Clough–Penzien spectral model was fitted to the specific barrier model of Papageorgiou and Aki (1983, 1985, 1988). The power spectral density of earthquake input motion based on the modified Clough–Penzien model is shown in Fig. 2. Table 1 lists parameters of a second-order linear low-pass filter of the modified Clough–Penzien model described by the Eq. (27). The Mexico City 1985 earthquake was known to have dominant frequency content at about 0.5 Hz frequency and the peak ground acceleration of the Mexico earthquake was 0.17g. The modified Clough–Penzien spectral model fitted to the specific barrier model of Papageorgiou and Aki shows that extensive energy is distributed in the frequency range of 0–5 Hz. On the other hand, the most available major earthquake records exhibit that the energy is released in the much prolonged frequency range. The behavior of base-isolated structures subjected to the modified Clough–Penzien power spectrum and the Mexico earthquake obtained by this study and Su et al. are compared.

4. Verification of analysis results

4.1. Five degrees of freedom superstructure

The base-isolated building with six degrees of freedom is analyzed based on the proposed method. Extensive sensitivity analysis is performed to understand the behavior of superstructure isolated with resilient-friction base isolator (R-FBI) system. The important parameters include natural vibration period of base isolator and superstructure, damping ratio of base isolator and superstructure. Table 2 summarizes the structural parameters used in this analysis.

4.2. Analysis results

The spectral densities of the relative displacement response for the input motion described by the modified Clough–Penzien model can be derived from Eq. (11) and Eq. (24). They are plotted in Fig. 3. ζ_b and ζ_e are the damping ratio of base isolator and equivalent

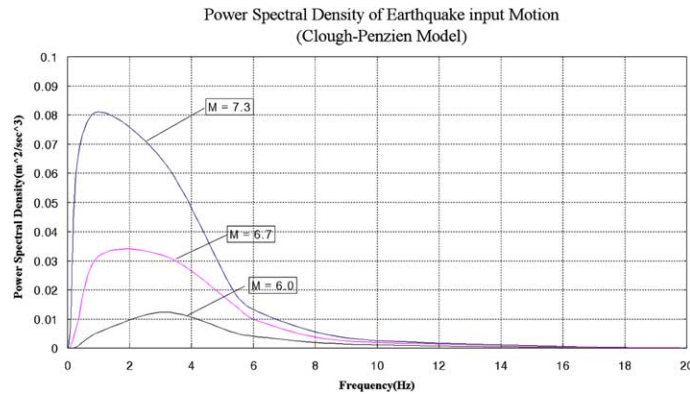


Fig. 2. Power spectral density of earthquake input motion (modified Clough–Penzien model).

Table 1

Parameters of modified Clough–Penzien spectral model fitted to different spectra

M (1)	$\log M_0$ (dyne-cm) (2)	S_0 (cm^2/s^3) (3)	f_c (Hz) (4)	ζ_c (5)	f_g (Hz) (6)	ζ_g (7)	f_m (Hz) (8)	ζ_m (9)
<i>Specific barrier model (Papageorgiou, 1988)</i>								
7.3	27	865.80	0.17	1.0	4.03	3.56	3.56	0.71
6.7	26	336.43	0.34	1.0	6.48	2.98	5.05	0.71
6.0	25	134.88	0.80	1.0	4.79	0.75	10.22	1.42

Table 2

Parameters used for sensitivity analysis

Figures	Parameters considered for analysis
Fig. 3(a), (b)	$\zeta_1 = 0.05, \zeta_2 = 0.07, \zeta_3 = 0.10, \zeta_4 = 0.12, \zeta_5 = 0.14$ $\zeta_1 = 0.1, \zeta_2 = 0.14, \zeta_3 = 0.20, \zeta_4 = 0.24, \zeta_5 = 0.28$ $T_s = 0.5$
Fig. 4(a), (b)	$\zeta_1 = 0.05, \zeta_2 = 0.07, \zeta_3 = 0.10, \zeta_4 = 0.12, \zeta_5 = 0.14$
Fig. 4(c), (d)	$\zeta_e = 0.2, \zeta_b = 0.2, T_b = 2.0$
Fig. 5(a), (b)	$\zeta_1 = 0.05, \zeta_2 = 0.07, \zeta_3 = 0.10, \zeta_4 = 0.12, \zeta_5 = 0.14$
Fig. 5(c), (d)	$T_b = 2.0$
Fig. 5(e), (f)	
Fig. 6(a), (b)	$\zeta_1 = 0.05, \zeta_2 = 0.07, \zeta_3 = 0.10, \zeta_4 = 0.12, \zeta_5 = 0.14$ $T_b = 2.0, \zeta_e = 0.05$

damping of the linearized system, respectively. T_b and T_s are the fundamental vibration periods of a isolation system and superstructure, respectively. Damping ratios for the first mode through fifth mode used for the calculation of spectral densities of displacement response of superstructure are listed in Table 2. The values of 10% and 20% for both ζ_b and ζ_e are considered in this analysis in which the 2s as natural periods of base isolator are used.

Magnitudes of power spectral density of displacement response of fixed-base superstructure are compared with those of the isolated superstructure in Fig. 3(a), indicating that base isolator absorbs the most displacement of superstructure. It is also noted that the

shift of natural vibration period of an isolated system indicates that base-isolation provides more flexible isolated system as depicted in the shifted effective frequency of the entire system, i.e., superstructure plus base-isolated system. It is also found that displacement response of the fixed-base structure is sensitive to the change of the damping ratio of the structure while that of the superstructure with isolator does not respond sensitively to the change of structural damping. Eqs. (21) and (24) yield the spectral density of absolute acceleration response. Fig. 3(b) shows that acceleration response obtained for superstructure without isolator is considerably larger than that of a base-isolated superstructure. As in the case of displacement responses, the

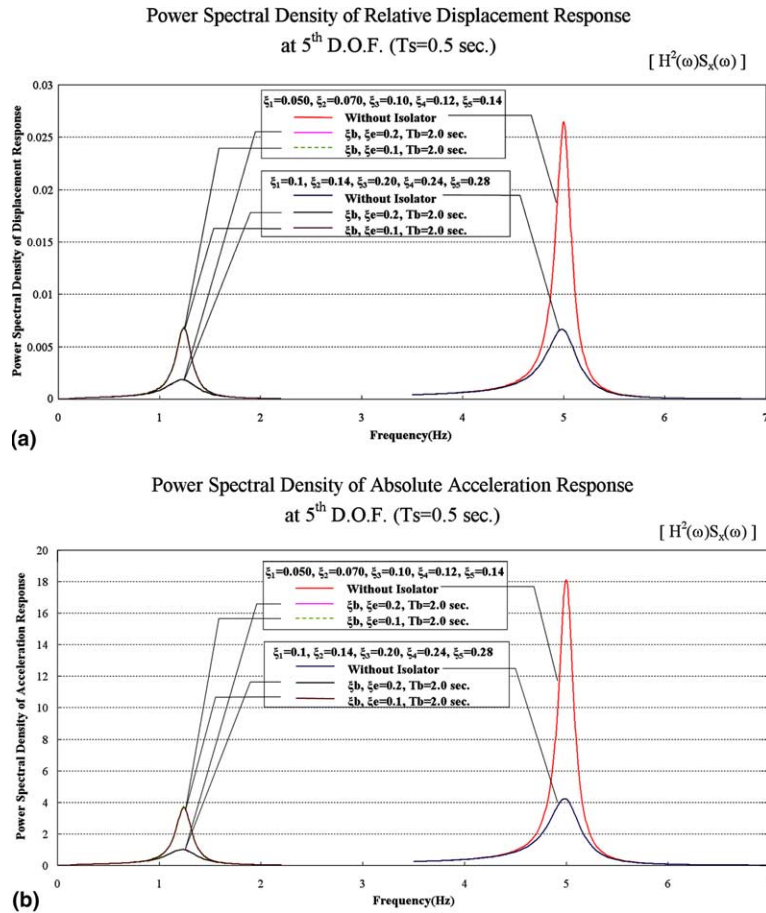


Fig. 3. (a) Power spectral density of relative displacement response at 5th DOF ($T_s = 0.5$ s); (b) Power spectral density of absolute acceleration response at 5th DOF ($T_s = 0.5$ s).

acceleration of the fixed-base structure is very sensitive to the change of the damping ratio of a superstructure. The considerable reduction of the peak response of superstructures can be obtained as both the damping ratio of the base isolator system and the equivalent damping of linearized system increase. Even though the base isolator is responsible for the primary mitigation of the acceleration, considerable acceleration is absorbed by superstructure.

Fig. 4(a)–(d) show spectral densities of displacement and acceleration responses of both the superstructure and isolator for the different flexibilities of superstructures. In these figures the spectral densities are plotted against natural period of superstructure (T_s) varying 0.1s through 2.0s. It is found that area of the density curve representing the magnitude of both displacement and acceleration response of base-isolated structures decreases as the superstructure becomes stiff.

An extensive sensitivity analysis is carried out to investigate the behavior of base-isolated structures.

When the natural periods of base isolator and the superstructure are both 2s, the base-isolated structure can be treated as the fixed structure with natural period of 2s. Fig. 5(a) and (b) show that the displacement and acceleration responses of the base-isolated structure with natural period of 2s for both the isolator and the superstructure are found to be the same as those of fixed structure with natural period of 2s for the damping higher than 15% of base isolator and equivalent damping of the linearized system. Slight differences are noticed for the damping ratio lower than 15% as shown in Fig. 5(a) and (b). The relative responses at 5th DOF and isolator are compared in Fig. 5(c) and (d), showing the influence of the stiffness of the superstructure on the reduction of base-isolated structures. It can be found from Fig. 5(c) that the isolator takes major displacement response for the natural period less than 1s of superstructure. Even if the structure is isolated at base the displacement response of the superstructure increases rapidly when the superstructure becomes flexible with

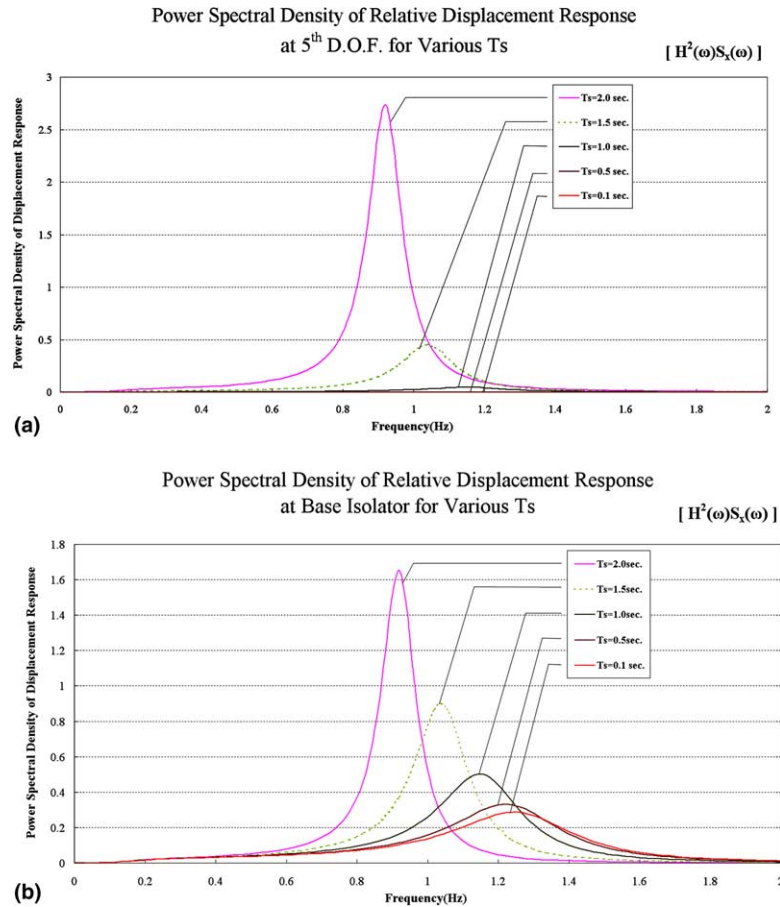


Fig. 4. (a) Power spectral density of relative displacement response at 5th DOF for various T_s ; (b) Power spectral density of relative displacement response at base isolator for various T_s ; (c) Power spectral density of absolute acceleration response at 5th DOF for various T_s ; (d) Power spectral density of absolute acceleration response at base isolator for various T_s .

the natural period longer than 1.5 s. This indicates that the base isolator does not play a significant role to absorb seismic energy when the superstructure is too flexible. These figures will help to determine the optimum stiffness range of the superstructure for the seismic isolation. The effective reduction of displacement response is expected for the range of 0.5 s through 1 s of natural period of superstructure for any damping ratio. The accelerations at 5th DOF and isolator are compared in Fig. 5(e) and (f). Fig. 5(c) and (e) indicate that the displacement and acceleration response of isolator exhibit relatively slight variation compared with superstructure for the change of the natural period of superstructure.

However, the damping ratio of base isolator and equivalent damping of the linearized system are some of the most important parameters that affect both the displacement and acceleration of isolator as can be seen in Fig. 5. Unlike the displacement, the acceleration response of the almost equal magnitude is transmitted to

both the superstructure and isolator as shown in Fig. 5(e) and (f). Various types of sensitivity analysis are now possible at a reasonable time and the corresponding cost. Fig. 6 demonstrates the influence of stiffness of the superstructure on the displacement and acceleration of the base-isolated structure as a function of the damping of base isolator. Fig. 6(a) shows that the rapid reduction of the displacement of isolator is obtained as the isolator damping increases for all natural period of superstructure. The isolator damping does not show much influence on the reduction of the displacement of the stiff superstructure, for proper periods shorter than 1.0 s. It is, however, clearly noted that base isolator can reduce the displacement response more effectively when superstructure becomes stiff enough as shown in Fig. 6(a). It is also found from Fig. 6(b) that the isolator damping and the stiffness of the superstructure are the key parameters to reduce the acceleration of the base-isolated structure. The acceleration response decreases as the iso-

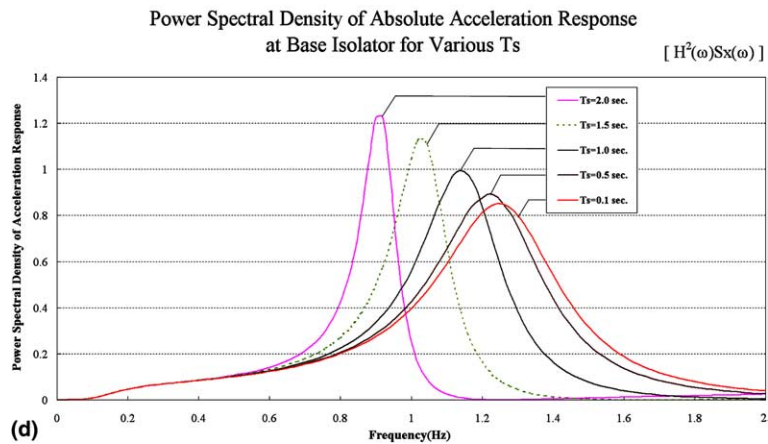
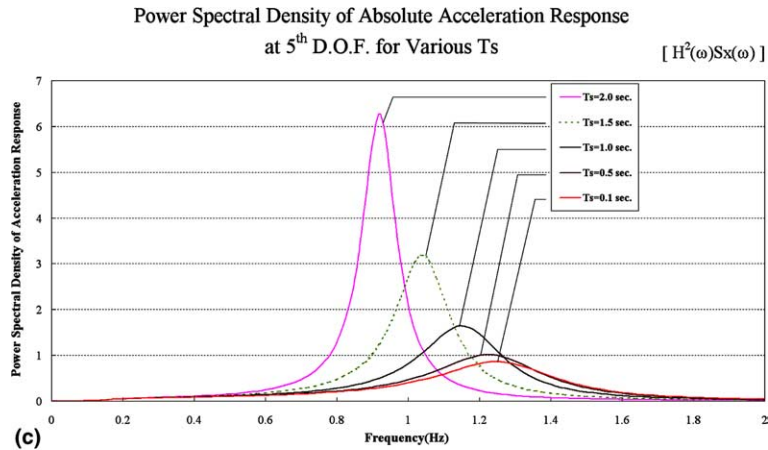


Fig. 4 (continued)

lator damping increases for all range of the natural period of a superstructure. A fast preliminary design is, therefore, possible. A reasonable stiffness of the superstructure and the ratio of isolator damping can be determined based on Fig. 6.

Su et al. [6] used a fourth-order Runge–Kutta–Gill numerical technique for integrating the equations governing the modal amplitude of shear frame structure. In their study peak responses of shear frame structure isolated with various base isolation system subjected to several earthquake ground input motions were calculated. The peak responses of structures isolated with R-FBI system of the present study are compared with the behavior of the Mexico earthquake obtained from Su et al. as shown in Fig. 5. Su et al. performed an analysis in the time domain, and therefore the comparison with this represents a validation of the proposed procedure. Similar responding trend of peak relative displacement and absolute acceleration are clearly observed between the results of present investigation and Su's work although the magnitude of relative displacement

and absolute acceleration can not be directly compared since the structures are subjected to different magnitude of ground input motions. For the isolated structure, the displacement of both the superstructures and isolator increases as superstructures becomes more flexible. This trend is true for both the present study and Su's study as shown in Fig. 5(a) and (c).

5. Conclusions

The analysis method based on frequency domain is proposed to seek the peak responses of structure isolated with R-FBI system, recognizing that time history analysis based method for the analysis of base-isolated structure requires extensive computational effort as well as time. The performances of multi-story structures isolated with the resilient-friction isolation (R-FBI) system are evaluated by an equivalent linearization technique. Effective analytical approach is proposed to calculate complex frequency response functions of N degrees of

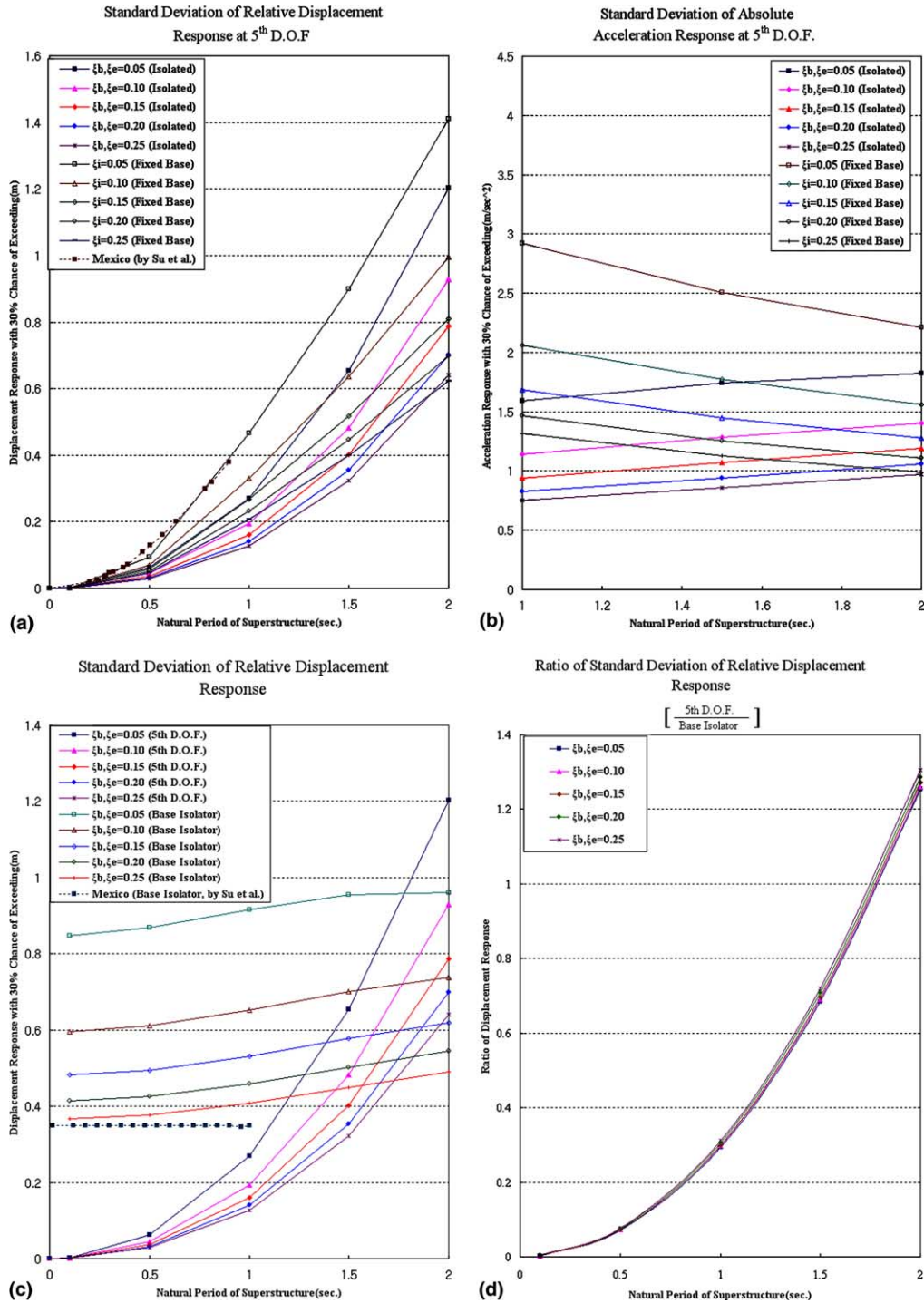


Fig. 5. (a) Standard deviation of relative displacement response at 5th D.O.F.; (b) Standard deviation of absolute acceleration response at 5th D.O.F.; (c) Standard deviation of relative displacement response; (d) Ratio of standard deviation of relative displacement response; (e) Standard deviation of absolute acceleration response; (f) Ratio of standard deviation of absolute acceleration response.

freedom systems. The excitation–response relations for stationary random process are then accurately formu-

lated to estimate responses of base-isolated structures. The results obtained from the analysis of frequency do-

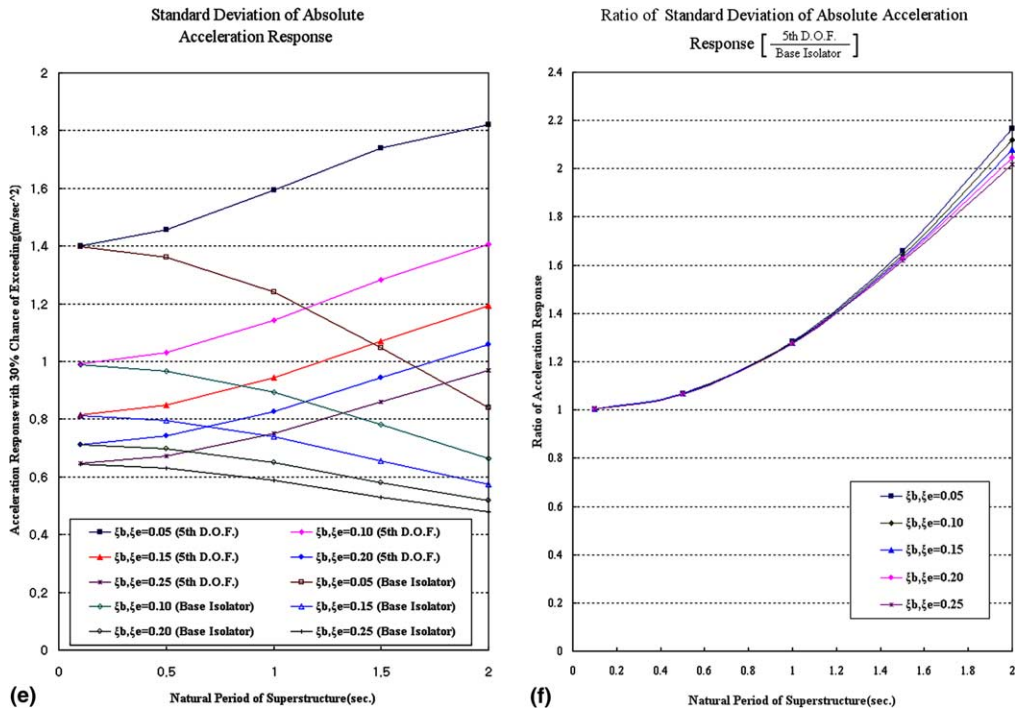


Fig. 5 (continued)

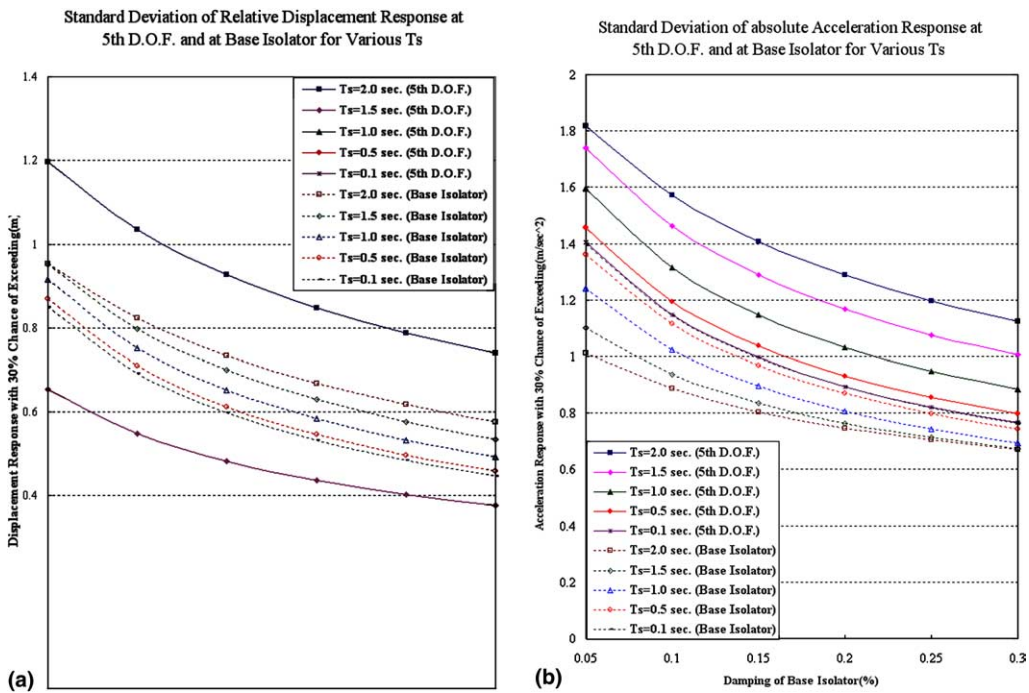


Fig. 6. (a) Standard deviation of relative displacement response at 5th DOF and at base isolator for various T_s ; (b) Standard deviation of absolute acceleration response at 5th DOF and at base isolator for various T_s .

main are compared with those obtained from Su's work. The summarized findings and characteristics of relative displacement and acceleration for the variations of the important structural parameters are as follows.

- (1) Extensive sensitivity studies to find the influence of various important structural parameters of both isolator and superstructure on the behavior of structures isolated with R-FBI system are possible by the simplified method proposed in this study. The important design parameters including optimal stiffness of the superstructure and the damping ratio of isolator can be determined, quickly and accurately.
- (2) Both the displacement and acceleration response of a superstructure without isolator is much more sensitive to the change of the damping ratio of the superstructure while the displacement and acceleration responses of a superstructure with isolator are not significantly influenced by structural damping.
- (3) Increasing the damping ratio of base isolator and equivalent damping of linearized system can more effectively reduce displacement and acceleration of superstructures than increasing the natural period of base isolator.
- (4) The base isolator is more effective to mitigate displacement than acceleration. Superstructure takes relatively considerable acceleration response, while only small displacement can be experienced by superstructures especially for stiffer superstructures ($T_s < 1$ s.).
- (5) The displacement and acceleration response of isolator does not exhibit any notable variation for the change of the natural period of superstructure, but the damping ratio of base isolator and equivalent damping of the linearized system are important parameters that affect both the displacement and acceleration of an isolator.
- (6) The reduction of the displacement of flexible superstructures (natural period larger than 1.0 s) can be effectively achieved by increasing the isolator damping. Conversely, the displacement of stiff structures is not influenced by the variations of the isolator damping. However, the acceleration response decreases as the isolator damping increases for all range of the natural period of superstructure.
- (7) The behavior of base-isolated structures of this study subjected to the modified Clough–Penzien spectral model fitted to the specific barrier model of Papageorgiou and Aki fits well with the behavior of the Mexico earthquake obtained from the time domain analysis by Su et al.

Acknowledgments

The authors would like to thank Kyung Hee University for the generous sharing of information and facilities relevant to this research. Financial support provided by Kyung Hee University is also gratefully acknowledged.

References

- [1] Mostaghel N. Resilient-friction base isolator. Report No. UTEC 84-097. University of Utah Salk Lake City, Utah, 1984.
- [2] Mostaghel N, Hejazi M, Khodavvedian M. Responses of structures supported on resilient-friction base isolator. In: Proceedings of the Third US National Conference on Earthquake Engineering, Charleston, SC, 1986. p. 1993–2003.
- [3] Mostaghel N, Khodavvedian M. Dynamics of resilient-friction base isolator (R-FBI). *Earthquake Eng Struct Dynam* 1987;15(3):379–90.
- [4] Su L, Ahmadi G, Tadjbakhsh IG. A comparative study of base isolation systems. Report No. MIE-150. Clarkson Univ. Potsdam, NY, 1989.
- [5] Gueraud R, Noel-Leroux JP, Livolant M, Michalopoulos AP. Seismic isolation using sliding elastomer bearing pads. *Nucl Eng Des* 1985;84(3):363–77.
- [6] Su L, Ahmadi G, Tadjbakhsh IG. Performance of sliding resilient-friction base-isolation system. *J Struct Eng, ASCE* 1991;117(1):165–81.
- [7] Booton RC. The analysis of nonlinear control systems with random inputs. *IRE Trans Circuit Theory* 1954;1:32–4.
- [8] Kazakov IE. Approximate probability analysis of operational precision of essentially nonlinear feedback control systems. *Auto Remote Control* 1956;17:423.
- [9] Caughey TK. Equivalent linearization technique. *J Acoust Soc Amer* 1963;35(11):1705–11.
- [10] Spanos P-TD. Stochastic linearization in structural dynamics. *Appl Mech Rev* 1981;34:1–8.
- [11] Caughey TK. On the response of non-linear oscillators to stochastic excitation. In: Huang TC, Spano PD, editors. *Random vibrations*. New York: American Soc. Mech. Engrs.; 1984. p. 9–14.
- [12] Caughey TK. On the response of non-linear oscillators to stochastic excitation. *Probab Eng Mech* 1986;1:2–4.
- [13] Su L, Ahmadi G. Earthquake response of linear continuous structures by the method of evolutionary spectra. *Eng Struct* 1988;10(1):47–56.
- [14] Fan F, Ahmadi G. Random response analysis of frictional base isolation system. *J Eng Mech Div ASCE* 1990;116(9):1881–901.
- [15] Lin BC, Tadjbakhsh IG, Papageorgiou AS, Ahmadi G. Performance of earthquake isolation systems. *J Eng Mech Div ASCE* 1990;116(2):446–61.
- [16] Constantinou MC, Tadjbakhsh IG. Response of a sliding structure to filtered random excitation. *J Eng Struct Mech* 1984;12(3):401–18.

- [17] Papageorgiou AS, Constantinou MC. Response of sliding structures with restoring force to stochastic excitation. *J Probab Eng Mech* 1990;5(1):19–34.
- [18] Su L, Ahmadi G, Tadjbakhsh IG. A comparative study of performances of various base isolation systems—part I/ Shear frame structures. *Earthquake Eng Struct Dynam* 1989;18:11–32.
- [19] Crandall SH, Mark WD. Random vibration in mechanical systems. Academic Press; 1973.
- [20] Basu B, Gupta VK. Wavelet-based non-stationary response analysis of a friction base-isolated structure. *Earthquake Eng Struct Dynam* 2000;29(11):1659–76.
- [21] Khechfe H, Nori M, Hou Z, Kelly JM, Ahmadi G. An experimental study on the seismic response of base-isolated secondary systems. *J Press Vess Technol, American Society of Mechanical Engineers* 2002;124(1): 81–88.